D. A. Chance
J.-C. A. Chastang
V. S. Crawford
R. E. Horstmann
R. O. Lussow

HeNe Parallel Plate Laser Development

A parallel plate format is used for fabricating "hard" sealed HeNe lasers. The new packaging geometry and construction process are suitable for large scale manufacturing. Cut plate, molded plate, and folded beam lasers have been built and tested. Several changes from conventional lasers, such as evaporated film cathode and anode, square cross section bore, glass sealed Brewster windows, and "soft" glass bore materials, are discussed. The power output capability, measurements of gain and loss parameters, and the reliability of these lasers are also considered.

Introduction

In the early experimental designs of the HeNe laser [1, 2], the emphasis was on obtaining operating models. As a result, geometrical considerations such as bore dimensions, straightness, and alignment were paramount concerns. Permanently sealed gas volumes, compact structures, long cathode lifetimes, rigid optical cavities, etc., soon became important as the need for commercial HeNe lasers developed. The emphasis shifted to ease of operation, reliability, long lifetime, and lower cost.

Elaborate alignment schemes are still important in high power gas lasers where long bores are necessary. Small, low power lasers are typically of the sidearm variety or of the more rigid coaxial type [3] currently preferred in commercial designs and shown in Fig. 1. The basic structure of the coaxial type consists of a bore coaxially located within an outer cylindrical metal cathode. In most of these lasers, the bores extend into (and are terminated within) the cathodes. One advantage of these structures is that they require the use of only conventional glass tubing. Another advantage is even distribution of the current to the cathode, resulting in reduced likelihood of "hot spots" on the cathode.

The coaxial laser has disadvantages from both the structural and the ease of manufacturing points of view. Structurally, the cantilevered bore may be deformed during laser operation, when the bore surface may reach a temperature of 200°C. Another structural concern is the fragility of the orthogonal support of the bore.

In efforts to strengthen the lasers and avoid bore sag, ingenious schemes were devised for providing at least two points of support for the bore. Two such schemes currently used are shown in Figs. 2 and 3. In Fig. 2 a slip joint is provided at the end of the bore. Some tolerance is required on the diameter of the outer sleeve to allow for thermal expansion of the bore during operation, and this tolerance permits lateral movement of the bore. As will be described subsequently, the bore ends are the apertures that define diffraction losses. Any change in the position of the limiting aperture drastically affects power output. In the complex structure shown in Fig. 3, the bore is supported in a pressed sleeve where it is normally joined as a ring seal. In a third design, additional support for the bore is provided by additional ring seals and support webs from the coaxial tube to the bore. Thermal expansion problems as a result of the temperature difference between the bore and outer tube occur in this structure. In the fabrication of any of these structures, precautions are necessary in order to maintain bore straightness.

Large scale manufacturing of gas lasers is hindered by reliance on conventional glass blowing technology. Attempts to use machined metal parts were not particularly successful. For example, the use of anode end caps resulted in large anode capacitances and plasma instabilities, whereas aluminum cathode envelopes were difficult to seal to glass parts.

In effect, coaxial gas lasers do not readily lend themselves to large scale fabrication methods, and their stability and ruggedness are sometimes questionable. Efforts to alleviate these problems have been successful, but at high costs. This paper describes our experience with an alternative to the coaxial gas laser, a parallel plate design. This structure is especially suitable for mass fabrication, is rugged, and promises reliability advantages not now present in gas lasers. The proposed laser is fabricated without the need for glass blowing; instead, techniques already developed by gas panel display manufacturers [4, 5] are used. A strikingly similar and independent effort was reported by Fein and Salisbury [6].

In this paper we discuss practical considerations in HeNe laser design and fabrication. We then consider fabrication of the parallel plate gas laser, including bore considerations, sealing and filling, a variant called the molded structure, and optical design. Finally we discuss performance of the parallel plate laser, including its reliability.

Practical factors in HeNe laser design and fabrication

Depending upon its intended use, design alternatives for the output of a HeNe laser, besides a certain power level, may include multimode or single mode (generally TEM_{00}) structure, large or minimal divergence, and undefined or defined (generally linear) polarization properties. A constant level of power output is also desired and is the result of stable operating conditions. Most important are the stability of the laser resonator, as well, of course, as the plasma discharge.

A laser resonator is defined by two mirrors and the associated bore. In this context we mean bore to refer only to that portion of the constricted plasma channel through which current flows. Alignment consists of making the optical axis, as defined by the line which joins the center of curvature of the mirrors, coincident with the bore axis within prescribed tolerances (typically 10^{-3} radian). The dimensional stability of the laser structure should be sufficient to make alignment permanent once established.

Most HeNe lasers are designed for TEM_{00} output. This is done by setting diffraction losses at a level such that only this mode is self-sustaining. The diffraction losses are generally considered to be defined by limiting aper-

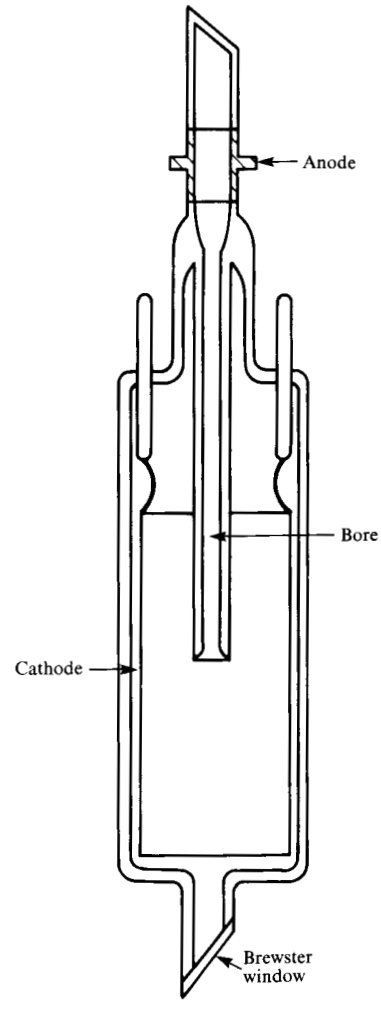

Figure 1 The coaxial laser.

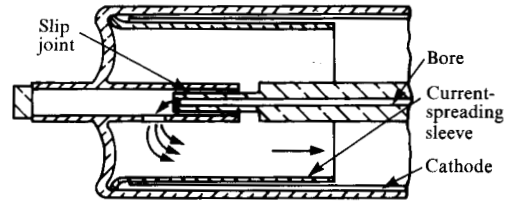

Figure 2 Slip joint support for laser bore.

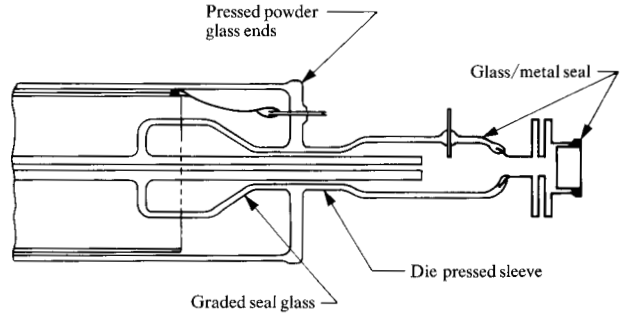

Figure 3 The coaxial laser with die pressed sleeve for bore support.

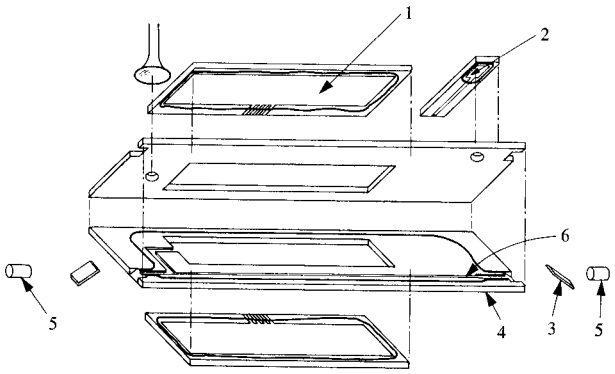

Figure 4 Schematic of the multiplate laser: 1, upper cathode; 2, anode; 3, Brewster window; 4, lower bore panel; 5, mirrors; and 6, bore.

Table 1 Factors affecting power output.

Loss	*Power change*
Diffraction loss increase at the limiting aperture	Drastic
A second aperture becomes limiting	Drastic
The beam axis and plasma axis move away from each other	Mild
Gain	
Cathode sputtering resulting in burying of He and Ne atoms	Drastic
He loss by diffusion	Mild. Observable after thousands of hours
Gas impurity	
Negative ion forming	Drastic
Positive ion forming	Mild

tures, which are usually extremities of the bore. Once the laser is aligned, any appreciable change in the position of these apertures constitutes a misalignment, with increased diffraction losses and the output drastically affected.

The number of Ne atoms at the upper lasing level and the ratio of that number to those at the lower lasing level determine the first order gain of the laser bore. Any parameter change which affects these numbers significantly changes power output. The manner in which Ne atoms at the upper lasing level are created is now well understood [1, 7, 8]. Lasing has been obtained within a pressure range of 100 to 800 Pa, with optimum He:Ne ratios between 5:1 and 11:1 and bore currents of 2-5 mA/mm^2. In addition, the relation between bore diameter, d, and pressure for optimum power is given by the relationship [9, 10]

$$\frac{p(\text{Pa})}{d(\text{mm})} = 390 \text{ to } 530. \quad (1)$$

One may assume for first order consideration that He and Ne atoms are evenly distributed throughout the bore and that the distribution of lasing Ne atoms corresponds to the current distribution across the bore. This distribution is the zero order Bessel function for the circular bore and is a cosine function for the square bore [11]. For maximum power, therefore, beam alignment with the center of the bore is optimum. Table 1 summarizes the generally accepted factors affecting power output.

Parallel plate HeNe laser

We considered the HeNe laser for large scale manufacturing. Constraints were the utilization of well known manufacturing methods, interchangeable parts, batch fabrication, and a gas volume that is completely "hard" (i.e., glass) sealed. These considerations were very much like those of Fein and Salisbury [6], but we placed more emphasis on completely hard seals. The parallel plate laser fabrication process was based on knowledge gained from gas panel fabrication [12, 13]. Desirable plasma densities in a bore and on a cathode were obtained by creating the necessary cavities for current flow in the glass structure. Thin film cathodes and anodes were obtained by the deposition of aluminum and other metals through masks.

Two types of parallel plate lasers were designed, fabricated, and tested. The first type, the multiplate laser, is shown in an exploded view in Fig. 4 and photographically in Fig. 5. In this design the cathode chamber was obtained by cutting out areas from one or more glass plates. The cut plate is sandwiched between other plates by means of glass seal techniques adopted from gas panel fabrication. Brewster windows are glass sealed into slots ground in the ends of the glass plates.

The second type of laser is the molded plate design shown in Fig. 6. This laser is fabricated from only two plates of glass, one of which is molded to form cathode and anode chambers of desirable dimensions.

In gas panel fabrication, the materials used and the seal processes are designed around the use of soda lime float glass with matching expansion lead glass for seals. We used similar materials and processes for fabricating parallel plate lasers. Brewster window glass was BK7 with a thermal expansion coefficient of 8.7×10^{-6}/°C.

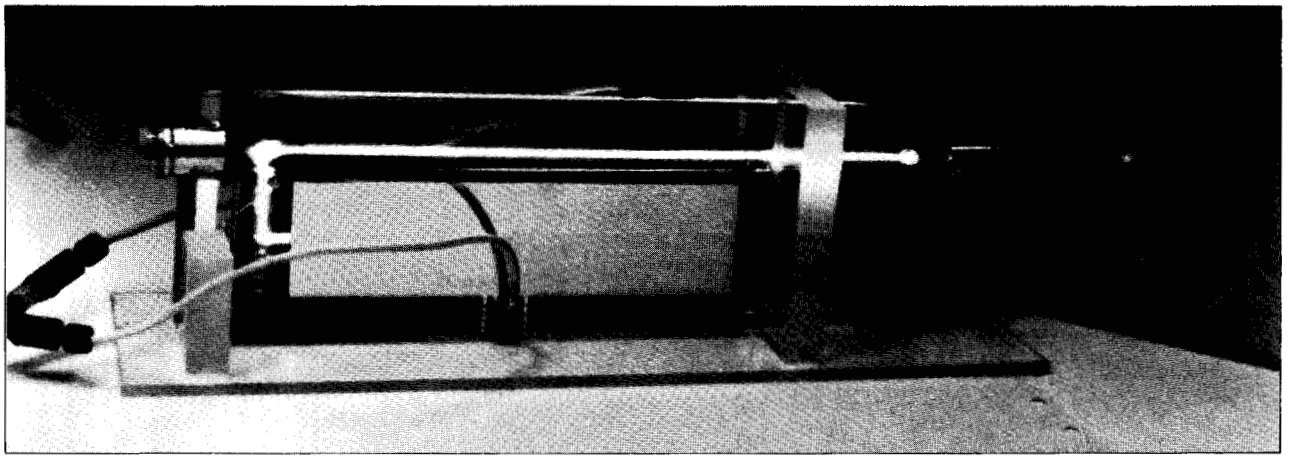

Figure 5 Photograph of the lasing multiplate laser.

Fabrication methods

Bore considerations

As previously mentioned, the bore in the parallel plate laser is fabricated by cutting a channel in one glass plate as shown in Fig. 4. The usual procedure is to use a diamond-impregnated wheel to traverse the plate with control on the depth of cut. Such a procedure enables one to obtain a bore of uniform cross section with relatively smooth walls. The bore is then completed by enclosing the channel with a second glass plate which is bonded in place, as shown in Fig. 4. It follows that one could design and fabricate a bore cross section to fit closely the laser beam configuration. Such a bore could measurably increase efficiency and output power for a given laser length [14].

Also, as indicated previously, the straightness of the plasma bore is a critical factor in laser fabrication. Typical machined tolerances are less than 2.5×10^{-2} mm for bore lengths up to 300 mm. Bore curvature follows naturally the curvature of the glass plates after the two plates have been sealed together by a high temperature process. Thus, the flatness of fixtures used in the seal process is a critical factor. Straight bores are the result of flat plates sealed together without camber. Diffraction losses are then at a minimum, the lasers are easy to align, and there is high output power.

In the bore of the laser, the ground glass surface is exposed to an inert gas plasma, and thus there is concern for possible material degradation. Likewise, there is possible exposure of the lead-based solder glass to the plasma. Neither of these concerns caused problems in lasers which were properly baked out to 300°C and filled with clean HeNe gas.

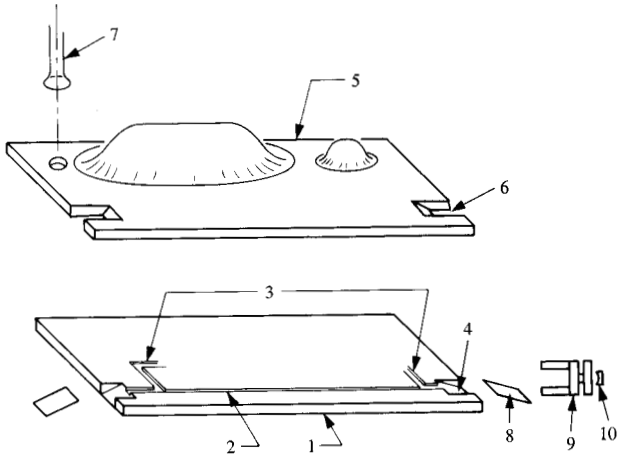

Figure 6 Schematic of the molded plate laser: 1, base panel; 2, bore; 3, anode and cathode connecting channel; 4, 6, Brewster window seat; 5, upper molded panel; 7, tip-off tube; 8, Brewster window; 9, mirror adjust fixture; and 10, mirror.

Cathode chamber

The cathode chamber for lasers which are fabricated with a large area cut out of a plate is completed by enclosing this area with plates on which the cathode is deposited. The process requires the use of seal glass which bonds effectively to glass as well as electrical feed-throughs to external leads.

A large cathode chamber is desirable to provide an adequate gas volume which minimizes pressure changes due to the loss of gases. Likewise, a large gas volume dilutes any contaminant gas that might be present. The geometrical shape of the chamber is generally designed to provide uniform distribution of the plasma over the cathode sur-

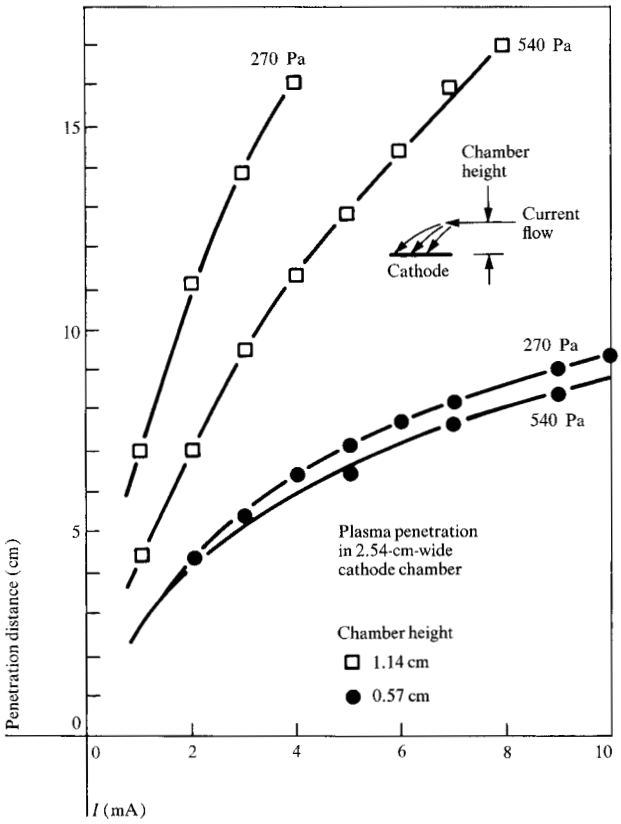

Figure 7 Plasma spread over Al cathode.

face. The spread of a HeNe plasma over Al thin film cathodes in parallel plate chambers 25.4 mm wide is shown in Fig. 7. It is observed that the distance to which the plasma extended on the cathode surface, and thus the cathode current density, are strong functions of both gas pressure and chamber height.

The optimum structure should be as symmetrical as possible with respect to the heated plasma bore so that distortions due to temperature gradients are minimized. Such structures are possible with duplications of either the cathode chamber or bore. Alternate designs where the anode and cathode chambers are placed at the ends of the bore result in relatively long structures.

Thin film cathodes and anodes

Deposited film electrodes (cathodes and anodes) have many advantages in the fabrication of the parallel plate laser. Electrical feed-throughs are fabricated as extensions of the metal electrodes and subsequently isolated from the gas chambers by seal glass. Surface machining and other cleaning procedures are not used, and alloy compositions may be fully optimized.

In the usual case of Al cathodes, evaporation or vacuum deposition is the simplest method of fabrication. Since the electrode areas do not require precisely defined edges, deposition through a mask is the usual method. Where alloy compositions are desired, both co-deposition of the various metals and layered depositions of the individual metals may be used. Layered depositions are subsequently diffused together during a high temperature process in which the structure is sealed together.

Contrary to the observations of Fein and Salisbury [6], no degradation of any anode material was observed with HeNe plasma in normal operation. Therefore, no effort was made to select or optimize an anode material. The anodes were simply co-deposited with the cathode using a mask for separation of the metallized areas.

The development of the thin film cathode for use in the parallel plate laser is discussed in a complementary paper by Chance et al. [15]. The plasma oxidation process of Hochuli et al. [16, 17] was found to clean organic contaminants from the cathode surface. In addition, surface oxide thickness was optimized for maximum resistance to sputtering while still allowing electron conduction. Al-Cu alloy showed best performance for reproducing surface characteristics which are optimized for long life.

Seal process

The seal process bonds all glass pieces into an integral unit containing anode and cathode chambers, interconnecting passageways, and the bore. The glass plates, Brewster windows, and tip-off tubing are cleaned in an ultrasonic bath to ensure the removal of all glass particles. Seal glass preforms are then prefired in position on the appropriate glass pieces. All pieces are then inserted in a fixture where they are held in their proper position and fired in a controlled temperature cycle. The seal glass softens and the glass pieces settle in their required location, thereby creating the integral laser unit. The materials chosen for fabricating the lasers are not particularly sensitive to the atmosphere during the seal process. At a seal temperature of 500°C, air or N_2 atmospheres have been used with success.

Details of a typical fixture are shown in Fig. 8. The flatness of the base platen is typically better than 2.5×10^{-2} mm over 300 mm. The upper platens apply weights to the seal areas resulting in uniform spread of the seal glass. The seals are normally 10 mm in width and less than 10^{-2} mm thick. The weight necessary to obtain good seals is approximately 10 g per linear mm of seal.

Skilled operators are not required for the seal process, since it is reduced to positioning glass pieces in a fixture.

The time required for such operations is short, and with sufficiently large belt furnaces large production volumes may be achieved. The seal fixture is not limited to individual lasers. The lasers may be arranged in stacks or several may be contiguously arranged in the same horizontal layer. In the latter case, individual lasers are separated after they have been sealed together.

Gas fill process

The gas fill and tip-off process is designed to ensure initial and continued purity of the HeNe plasma throughout the life of the laser. For the glass sealed, parallel plate laser, the problem is reduced to limiting outgassing from glass surfaces. One favorable factor is that likely impurity gases (e.g., N_2, O_2) are known to be gettered by Al cathodes [18].

The first step in the fill process is the plasma oxidation of the cathode. The cathode is operated in an oxygen plasma at 270 Pa and at current levels several times those used in the HeNe laser. The anode for this discharge is typically the supporting vacuum equipment. Current flows through the tip-off stem directly into the cathode chamber.

Following the oxygen discharge process, the laser is baked for several hours at 300°C to a vacuum greater than 10^{-5} Pa. On cooling, the laser is "burned in" with a HeNe plasma for several hours. Evacuation, final gas fill with pure HeNe gas, and tip-off complete the procedure.

Molded laser structure

The fabrication of the molded laser was an attempt to simplify the fabrication process by the use of only two panels of glass. In addition, by using a molded cathode chamber, we were able to locate the cathode surface symmetrically relative to the current flow. Referring again to the molded laser shown in Fig. 6, base panel 1 is machined to obtain the bore channel 2, the anode and cathode connecting channels 3, and the Brewster window slots 4. The molded panel 5 is also machined to obtain Brewster window slots 6. The other parts of the molded laser are the tip-off stem 7, the Brewster windows 8, the mirror attach fixtures 9, and the mirrors 10. The complete laser is shown in Fig. 9.

The molded panel and Brewster windows were fabricated from available materials which showed matching thermal expansion coefficients to soda lime glass. Similarly, the seal glass was selected for a seal temperature below the deformation temperature of soda lime glass and with matching expansion coefficient. Soda lime glass, the base panel material, was ordinary float glass for window applications. The molded panel was fabricated from

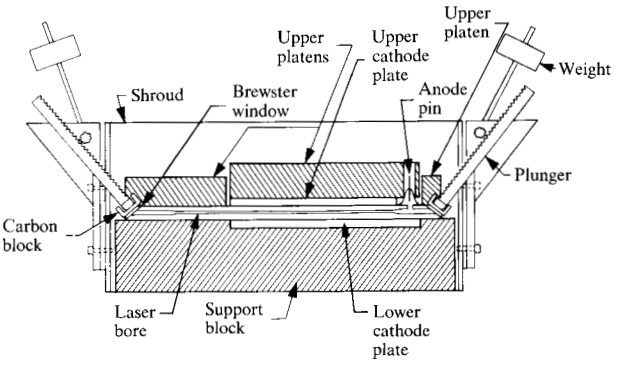

Figure 8 Typical fixture for glass seal process.

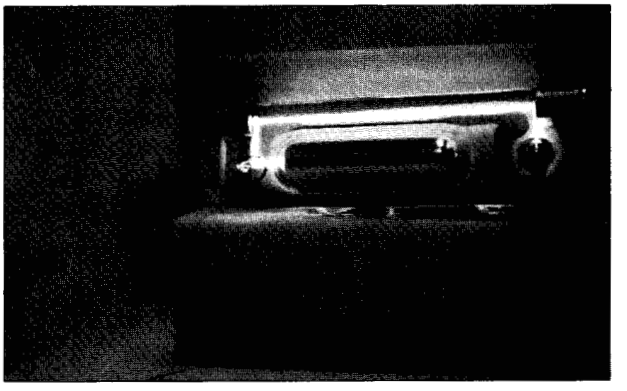

Figure 9 Photograph of a lasing molded laser.

Corning 0120 potash soda lead glass with an expansion of 8.9×10^{-6}/°C for 0–300°C. For the Brewster windows, the optical glass BK7 was used.

Optical design

Conventional HeNe lasers have bores with circular cross sections and, in general, unstressed Brewster windows. Parallel plate lasers have bores with square cross section and Brewster windows which are hard sealed and subject to stresses. As mentioned previously, the parallel plate laser is particularly amenable to multiple or folded bore configurations. These features have direct influence on the design and behavior of parallel plate lasers.

A laser with a bore cross section which is square exhibits diffraction losses which are different from those of conventional lasers, and the differences are experimentally determined below. The fact that Brewster windows are hard sealed may affect the output as well as the polarization characteristics of the laser. This question is examined in detail in a complementary paper by Chastang [19].

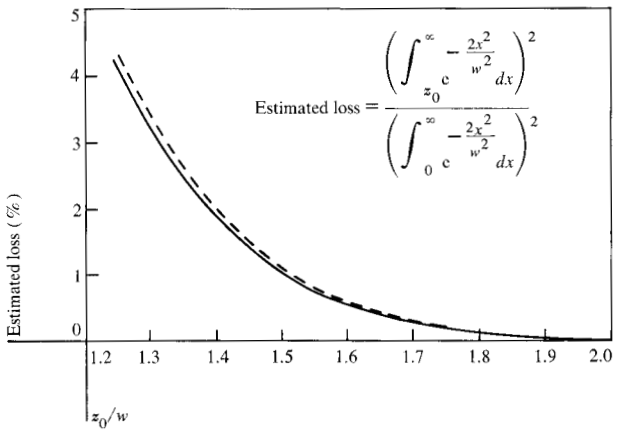

Figure 10 Change in diffraction loss between square and circular limiting aperture. (Dotted curve is for the square bore.) Parameter z_0 is the radius of a circular bore or 1/2 the side of a square bore.

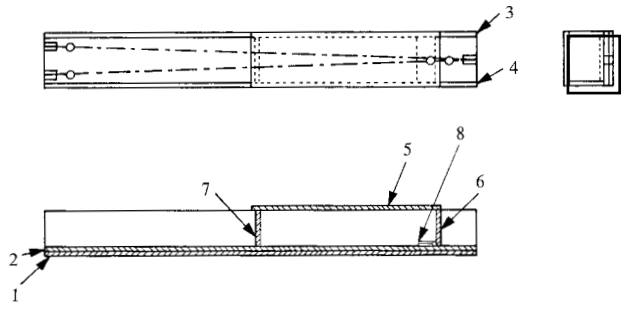

Figure 11 The folded beam laser: 1, base panel with bore; 2, upper panel; 3, 4, side support panels; 5, cathode panel; 6, 7, panels for enclosing cathode chamber; and 8, plasma directing panel.

The designers' goals are unchanged for the parallel plate laser. Given a certain number of constraints (overall length of structure, length of glass structure, length of active bore, availability of mirrors, etc.) one tries to trade off maximum power output in the TEM_{00} mode with alignment stability.

Laser fabrication results

Objectives

The initial parallel plate lasers were made for the purpose of determining the feasibility of fabrication concepts. After determining that parallel plate lasers could indeed be fabricated, experiments were designed to evaluate parameters in the power output equation. For example, practical measurements were made for determining diffraction losses at square-bore limiting apertures, as well as gain and saturation parameters by use of a folded bore laser. Finally, a molded laser structure was selected for evaluation of reproducibility and reliability factors.

Diffraction loss at a square limiting aperture

The estimated diffraction loss for a Gaussian [20] beam was calculated for a square bore and compared with the loss for a circular bore in Fig. 10. The results show that the difference in diffraction loss is of the order of 5% for the practical TEM_{00} laser with 1% diffraction loss.

Several methods were used to determine experimentally the diffraction loss of a square limiting aperture. These include the substitution of circular and square limiting apertures in the cavity of a multimode laser, movement of a square bore plasma within its optical cavity, and movement of the flat mirror of a near confocal cavity. The diffraction losses estimated from the power outputs showed negligible differences when the results for the circular and square limiting apertures were compared. Maximum difference estimated was 9%.

Gain and loss determination

The folded beam laser is an ideal instrument for the determination of unknown parameters in the power output equation for the parallel plate laser. The gain coefficient, total losses, and product of the average beam area and the saturation parameter were determined from the following considerations. Note that similar considerations may be made for two identical but independently powered bores which are properly aligned in series or parallel.

The power output equation may be written as follows [21]:

$$P = TW_0\bar{a}\left(\frac{g\ell/d}{A + T/2} - 1\right), \tag{2}$$

where P = power output, T = output mirror transmission, $W_0\bar{a}$ = saturation parameter × beam area, A = losses other than transmission, g = gain coefficient, ℓ = length of plasma in bore, and d = bore diameter. Rewriting Eq. (2),

$$A = \left(\frac{\ell/d}{\frac{P}{TW_0\bar{a}} + 1}\right) g - \frac{T}{2}. \tag{3}$$

The folded beam laser is now considered for a change in operating condition from lasing with the left bore plasma to lasing with plasma in both left and right bores. That is,

$$\left.\begin{aligned} \ell &\rightarrow 2\ell \\ P_L &\rightarrow P_{L+R} \end{aligned}\right\}. \tag{4}$$

Table 2 Measured parameters for the folded beam laser.

Radii of mirrors used			*He^4Ne^{20}, 7:1 Total pressure*	*Average $W_0\bar{a}$*	*Average gain, g*	*Average loss, A*
R_L (mm)	R_M (mm)	R_R (mm)	(Pa)	($\times 10^{-3}$ watt)	($\times 10^{-4}$)	(%)
1200	1200	1200	270	99.7	1.86	2.45
1200	1200	1200	200	108	1.88	2.39
1200	1200	1200	170	87.4	1.63	1.65
1200	∞	1200	270	127	2.47	3.6
1200	∞	1200	200	135	2.83	4.2
1200	∞	1200	170	122	2.92	3.9

All other parameters remain unchanged in Eq. (3). For the equation to satisfy both operating conditions, the coefficient of g must remain invariant. That is,

$$P_{L+R} = 2P_L + TW_0\bar{a} \tag{5}$$

and

$$W_0\bar{a} = \frac{P_{L+R} - 2P_L}{T}. \tag{6}$$

If $P_L \neq P_R$,

$$W_0\bar{a} = \frac{1}{T}(P_{L+R} - P_L - P_R). \tag{7}$$

The folded laser design is shown in Fig. 11, and its mirror configuration is schematically illustrated in Fig. 12. The effects on $W_0\bar{a}$ of various fill pressures and two different mirror configurations are summarized in Table 2. The configuration determines the mode volume, and it is observed that larger mode volumes result in higher values of $W_0\bar{a}$, as anticipated. The maximum value for W_0, assuming $\bar{a}$ = 1/5 area of bore, was found to be 24 watt/cm^2. This value is lower than the typical literature value of 30 watt/cm^2 [10]. Note, however, that $\bar{a}$ is expected to be less than 1/5 the area of the square bore and, consequently, W_0 higher.

We evaluated the gain coefficient and total loss for the system by varying the transmission loss in Eq. (3) and using the calculated results for $W_0\bar{a}$ above. If the individual bores show different power outputs and gains, then the following equations may be substituted for Eq. (3):

$$A = \left(\frac{\ell/d}{\frac{P_L}{TW_0\bar{a}} + 1}\right) g_L - \frac{T}{2}, \tag{8}$$

$$A = \left(\frac{\ell/d}{\frac{P_R}{TW_0\bar{a}} + 1}\right) g_R - \frac{T}{2}. \tag{9}$$

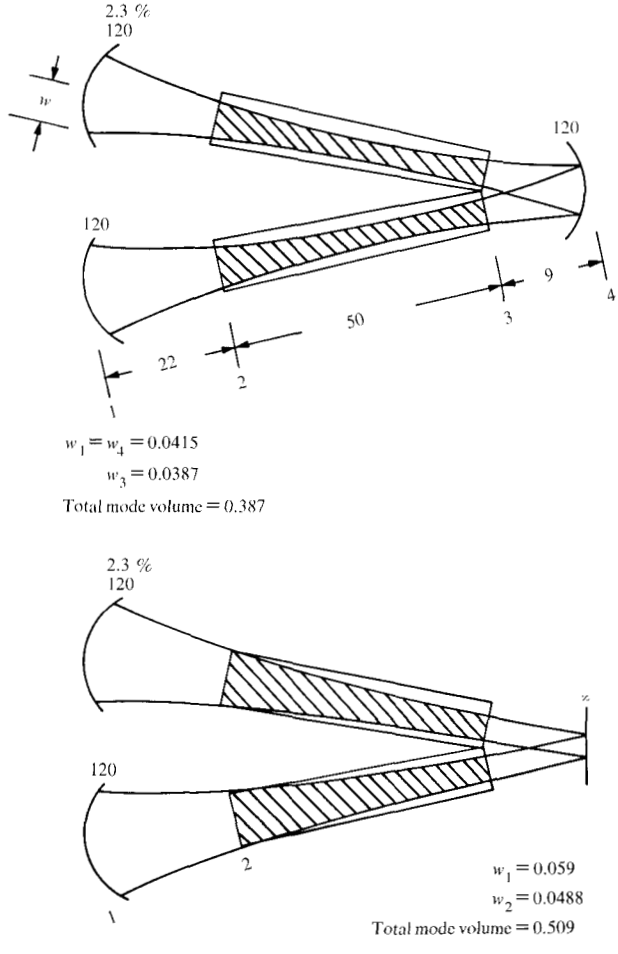

Figure 12 Mirror configurations in folded beam laser (dimensions are in cm).

The coefficients g and A were evaluated for the folded bore laser and are also shown in Table 2. The gain coefficient and total loss are observed to vary strongly with the

Table 3 Molded laser fabrication.

Laser #	*Brewster window*			*Seal glass overflow in bore*	*Bore cathode seal*	*Bore size* (mm)	*Miscellaneous*
	Brewster angle $(\theta_1)^\circ$	$(\theta_2)^\circ$	*Skew angle* (ϕ) (rad)				
M-6	56.63	56.14	0.001	None	Good	1.30	
M-7	57.86	58.78	0.013	~ 13 mm	Good	1.30	Quartz windows. Epoxy seal.
M-8	55.92	56.52	0.006	None	Good	1.29	
M-10	56.80	56.59	0.0	None	Good	1.30	
M-12	56.90	56.27	0.0	~ 25 mm	Good	1.30	
M-13	56.71	56.50	0.004	None	Open, ~ 19 mm	1.29	

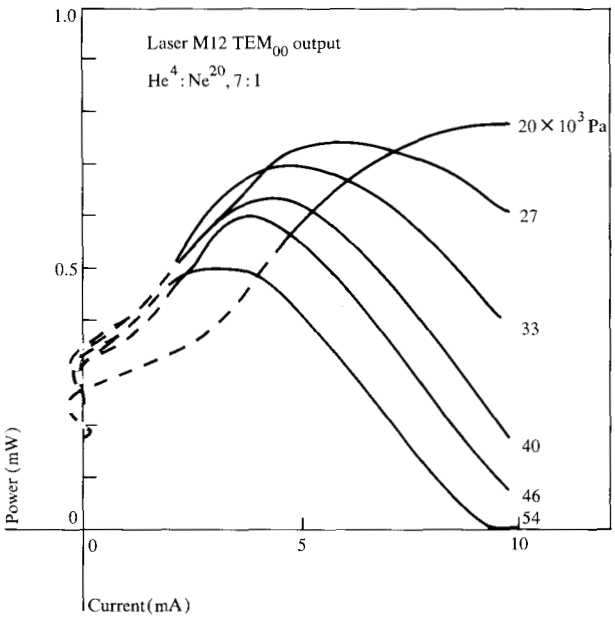

Figure 13 Typical power output for reproducible run lasers.

two different mirror configurations. This result is expected since a larger mode volume increases gain. In addition, more diffraction losses are expected for larger mode volumes, and larger total losses are expected. The values for the gain coefficient with a flat mirror at the apex varied from 2.47 to 2.92 $\times$ 10^{-4}, which is comparable to the nominal literature value of 3 $\times$ 10^{-4}. The relatively large losses observed are attributed to Brewster window losses. It is estimated that the reflection and birefringence loss at the Brewster windows is approximately 0.5% per window.

Molded laser fabrication

The results from the fabrication of seven lasers are summarized in Table 3, which shows the precision with which Brewster windows are glass sealed onto the laser structure. For a specified Brewster angle of 56.5°, the results showed a range of 55.9° to 56.9° and an average of 56.5°. The maximum skew angle, i.e., rotation of the window about the line it forms with the plane of incidence, was found to be 0.76°. Five lasers were fabricated with glass seals. A sixth structure was fabricated with epoxy sealed windows. Quartz windows were used in this structure in an attempt to isolate Brewster window problems that might be associated with the use of BK7. Seal glass overflow into two bores was observed, but no detrimental effects due to the overflow were detected.

The TEM_{00} output power of laser #M-12 is shown as a function of current and fill pressure in Fig. 13. This result was typical for the better lasers. A summary of maximum power outputs for TEM_{00} operation at 270 and 400 Pa is shown in Table 4. The maximum multiple mode output for glass-sealed BK7 windows with mirror radii of 600 mm was 2.1 mW. For epoxy-sealed quartz windows under similar conditions the output was 2.5 mW.

Reliability

The parallel plate laser has addressed three of the most common causes of failure in HeNe lasers—structural instability, changes in composition of the HeNe gas, and cathode sputtering.

Bore instability due to bending out of and within the horizontal plane is readily measured, since the bore is cut parallel to a flat surface and one edge of the plate. Accurate measurements in both bending directions during warmup showed changes less than 2.5 $\times$ 10^{-3} mm over 300 mm. These changes are well within allowable limiting aperture movement and adequate for alignment tolerance for the mirrors. Transient output power measurements showed changes attributed to the usual mode fluctuations and an exponential power rise to a maximum. The typical transient power output for good lasers is shown in Fig. 14.

Table 4 Molded laser operation. Mirror 1: radius = 1200 mm, transmission = 0.04%; mirror 2: radius = 300 mm, transmission = 0.9%.

Laser	*Pressure* (Pa)	*Max. Output Power* (mW) He^3:Ne^{20} 7:1	He^4:Ne^{20} 7:1	*Current* (mA)	*Comments*
M-6	270	0.15	0.1	6.0	0.52 mW observed initially
M-7	270	1.30	0.82	6.0	Quartz window, epoxy sealed
M-7	400	1.13	—	4.3	Tip-off fill
M-10	270	1.01	0.71	6.0	
M-10	400	0.89	—	4.5	Tip-off fill
M-12	270	1.0	0.75	6.0	
M-12	400	0.86	0.62	4.5	Tip-off fill
M-13	270	1.0	0.75	6.0	
	400	0.85	—	4.5	Tip-off fill

Table 5 Cathode sputtering in lasers.

Current (mA)	*Cathode chamber* *Type*	*Width* (mm)	*Closest distance from cathode to plasma entrance* (mm)	*HeNe pressure* (Pa)	*Sputtering observed*	*Time* (h)
6	Cut glass	50.8	5.71	270 to 400	Yes	~ 2000
6	Cut glass	50.8	11.4	270 to 400	No	> 8800
4.5 to 5.5	Molded	25.4	18.4	470 to 530	No	> 8800

The steady state leak rate of the glass sealed gas chamber is estimated to be of the order of 6.7×10^{-10} Pa-l/s and the critical time to achieve steady state flux approximately 10^7 hours. On the basis of these assumptions, the calculated impurity level after five years is estimated to be less than 10 ppm. Power degradation owing to leaks into and out of the properly constructed parallel plate laser was not anticipated nor detected. Good parallel plate lasers showed extremely stable and low noise output for thousands of hours. Power output change is less than 5% after 8800 hours.

The stable operation described above is compared with the operation of lasers which were fabricated with epoxy sealed Brewster windows. These lasers showed normal operation initially, but performance was degraded to very noisy outputs, a loss of 20% or greater of output power in 2000 hours, and the presence of a blue tinge in the plasma discharge at the entrance of the cathode chamber. The blue color is due to the presence of nitrogen, as indicated by spectral emission measurements [22].

Cathodes for HeNe lasers is the subject of a complementary paper [15]. Long lifetimes (thousands of hours) have been shown for optimized cathode material and chamber geometry. For cut plate lasers, cathode

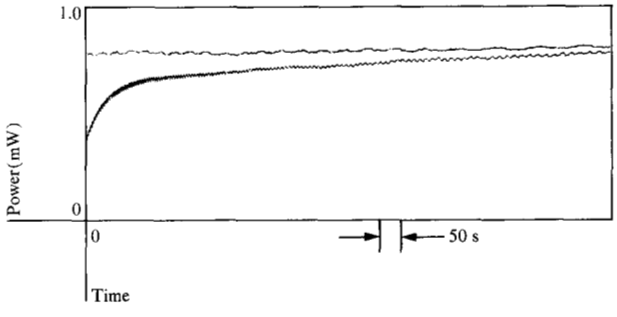

Figure 14 Cold start power output for molded laser structure. (Lower curve extends to upper curve.)

sputtering was observed after ~2000 hours of continuous operation for restrictive chamber geometries when the current entrance port is less than 6 mm from the cathode. The influence of chamber geometry and entrance port proximity to the cathode on the cathode current density is shown in Fig. 7. For properly designed chambers with entrance port to cathode distance greater than or equal to 11.4 mm, sputtering was not observed under normal operating conditions. Neither was sputtering observed in the molded laser. These results are summarized in Table 5.

Conclusions

Stable, long life HeNe lasers were fabricated in the parallel plate geometry using glass materials which are available in large quantities. Soda lime (C0080) and potash soda lead (C0120) glasses were used as bore materials with good results. Vacuum baking to 300°C is essential to reduce outgassing.

Thin film Al cathodes are readily deposited by evaporation and are not degraded by processes used in the fabrication of the laser. Glass seal to Al feed-throughs showed excellent leak-free seals. Reliability is excellent.

Fabrication of limited quantities of the parallel plate laser did not uncover any problems that may prevent fabrication on a large scale. Indeed, one may project very high laser yield owing to the absence of critical tolerances in the fabrication.

The molded cathode chamber is preferred to the cut glass chamber due to the symmetrical location of the cathode surface relative to the current flow and the use of fewer glass plates. Cathode thickness variations within the molded chamber of 1.5 to 3.0 μm did not affect reliability.

Replacing a Brewster window by a glass sealed mirror is a desirable improvement. A soda lime glass substrate with hard mirror coatings stable at 500°C is required. The use of only one Brewster window reduces considerably birefringence losses due to any strains in the Brewster windows.

Three complementary papers on important issues in the fabrication of gas lasers are included in this issue. The Al cathode, its less than 10^{-5}-mm oxide film, and changes observed during processing are discussed [15]. Optical concerns associated with hard sealed Brewster windows are presented in a second [19]. Finally, non-destructive testing of lasers by spectral emission measurements are discussed in a third [22].

Acknowledgments

The authors thank G. Messina for a superb fabrication effort on the molded lasers and J. Little for many valuable suggestions throughout the life of the project.

References

1. A. Javan, W. R. Bennett, Jr., and D. R. Herriott, "Population Inversion and Continuous Optical Maser Oscillation in a Gas Discharge Containing a He-Ne Mixture," *Phys. Rev. Lett.* **6,** 106–110 (1961). See also D. R. Herriott, "Optical Properties of a Continuous Helium-Neon Optical Maser," *J. Opt. Soc. Amer.* **52,** 31–37 (1962).
2. C. F. Luck, R. A. Paananen, and H. Statz, "Design of a Helium-Neon Gaseous Optical Maser," *Proc. IRE* **49,** 1954–1955 (1961).
3. W. P. Kolb, Jr., "Cold Cathode Gas Laser Discharge Tube," U.S. Patent Re 27,282, 1972.
4. P. H. Haberland, "Plasma Panels," *J. Vac. Sci. Technol.* **10,** 5 (1973).
5. D. Alpert and D. L. Bitzer, "Advances in Computer-based Education," *Science* **167,** 1582–1590 (1970).
6. M. E. Fein and C. W. Salisbury, "Integrated Construction of Low-Cost Gas Lasers," *Appl. Opt.* **16,** 2308–2314 (1977).
7. A. D. White and J. D. Rigden, "Continuous Gas Maser Operation in the Visible," *Proc. IRE* **50,** 1697 (1962).
8. W. R. Bennett, Jr., "Gaseous Optical Masers," *Appl. Opt.* **1,** 24–61 (1962).
9. E. I. Gordon and A. D. White, "Similarity Laws for the Effects of Pressure and Discharge Diameter on Gain of He-Ne Lasers," *Appl. Phys. Lett.* **3,** 199–201 (1963).
10. P. W. Smith, "On the Optimum Geometry of a 6328Å Laser Oscillator," *IEEE J. Quantum Electron.* **QE-2,** 77–79 (1966).
11. A. von Engel, *Ionized Gases*, Oxford University Press, London, 1965, p. 241.
12. A. Reisman and K. C. Park, "AC Gas Discharge Panels: Some General Considerations," *IBM J. Res. Develop.* **22,** 589–595 (1978).
13. A. Reisman, M. Berkenblit, and S. A. Chan, "Single Cycle Gas Panel Assembly," *IBM J. Res. Develop.* **22,** 596–600 (1978).
14. V. E. Privalov and S. A. Fridrikhov, "He-Ne Laser with a Conical Discharge Tube," translated from *Zh. Prikladnoi Spektroskopii* **12,** 937–939 (1970).
15. D. A. Chance, V. Brusic, V. S. Crawford, and R. D. MacInnes, "Cathodes for HeNe Lasers," *IBM J. Res. Develop.* **23,** 119–127 (1979, this issue).
16. U. Hochuli and P. Haldemann, "Cold Cathodes for Possible Use in the 6328 Å Single Mode HeNe Gas Lasers," *Rev. Sci. Instrum.* **36,** 1493–1494 (1965).
17. U. Hochuli, P. Haldemann, and D. Handwick, "Cold Cathodes for He-Ne Gas Lasers," *IEEE J. Quantum Electron.* **QE-3,** 612–614 (1967).
18. D. A. Chance, R. E. Horstmann, and V. S. Crawford, "Al-Mg Alloy for Reactive Gas Gettering in a Glow Discharge," *IBM Tech. Disc. Bull.* **18,** 3141 (1976).
19. J.-C. A. Chastang, "Polarization Problems of Parallel Plate Lasers," *IBM J. Res. Develop.* **23,** 132–139 (1979, this issue).
20. Arnold L. Bloom, *Gas Laser*, John Wiley & Sons, Inc., New York, 1968.
21. D. C. Sinclair and W. E. Bell, *Gas Laser Technology*, Holt, Rinehart and Winston, Inc., New York, 1969.
22. W. E. Ahearn and R. E. Horstmann, "Nondestructive Analysis for HeNe Lasers," *IBM J. Res. Develop.* **23,** 128–131 (1979, this issue).

Received August 24, 1978; revised October 27, 1978

D. A. Chance, J.-C. A. Chastang, V. S. Crawford, and R. E. Horstmann are located at the IBM Thomas J. Watson Research Center, Yorktown Heights, New York 10598. R. O. Lussow is located at the IBM Data Systems Division laboratory, East Fishkill (Hopewell Junction), New York 12533.